

Supporting Information

Zhou et al. 10.1073/pnas.1705927115

SI Materials and Methods

Plant Materials and Growth Conditions. A Kitaake rice mutant population containing 50,000 independent lines was generated by EMS-mediated mutagenesis. For blast-resistance screening, we used the blast fungus library containing 82 blast isolates (Dataset S5) to identify Kitaake-compatible blast isolates. We finally screened out seven Kitaake-compatible blast isolates (ZB25, Zhong1, Tetep, 99-20-2, 97-27-2, 0755-1-1, and ZE-1). Then the 50,000 independent lines were inoculated with mixed spores derived from the seven Kitaake-compatible blast isolates in field. Five mutant lines, including the *bsr-k1* mutant, showing enhanced disease resistance compared with wild-type Kitaake were obtained. To identify the *Bsr-k1* gene, we generated three F₂ populations of *bsr-k1* as the resistant parent crossed to the susceptible parents Kitaake and Joden, respectively. The three rice cultivars Shuhui527^{*bsr-k1/bsr-k1*}, Minghui63^{*bsr-k1/bsr-k1*}, and Mianhui725^{*bsr-k1/bsr-k1*} homozygous for the locus *bsr-k1* were developed by backcrossing Shuhui527, Minghui63, and Mianhui725 as receiver parents, respectively, with the *bsr-k1* mutant for six generations. These plant materials were grown in the fields at Sichuan Agricultural University in Wenjiang, Chengdu, or Pujiang, Chengdu, or Lingshui, Hainan, China.

Rice Blast and Bacterial Blight Disease Resistance Assays. Rice blast fungal spray inoculation assays, punch inoculation assays, and field trials assays were performed as described previously (21, 29). Rice bacterial blight inoculation assays were carried out using the leaf-clipping method as described previously (22). Briefly, rice plants were grown in the field normally until they were 6 wk old. Then the fully expanded leaves were clipped about 1 cm from the leaf tip using a pair of scissors dipped in the bacterial suspensions (OD₆₀₀ of 0.6). The lesion length and bacterial population accumulated in the inoculated leaves were measured 2 wk after inoculation.

Genetic Analysis and Map-Based Cloning of the *bsr-k1* Locus. The three F₂ populations derived from the crosses of Kitaake × *bsr-k1*, *bsr-k1* × Kitaake, and Joden × *bsr-k1* were used for the genetic analysis of the *bsr-k1* locus. The F₂ population derived from Joden × *bsr-k1* was also used to map the *bsr-k1* locus. We selected 995 F₂ plants which exhibited extreme resistance against blast isolate 99-20-2 in the F₂ population of the Joden × *bsr-k1* cross and verified the resistance by inoculation assay on their F₃ progeny. Bulk segregation analysis was first used to rapidly locate the *bsr-k1* locus on a chromosome. We then developed additional markers nearby the *bsr-k1* locus to construct the physical linkage map. For whole-genome resequencing, *bsr-k1* was backcrossed with Kitaake twice and was self-pollinated to produce BC₂F₄ progeny homozygous at the *bsr-k1* locus. Equivalent amounts of total DNA of 25 BC₂F₄ plants homozygous at *bsr-k1* were pooled and sequenced by Novogene at Tianjin, China. For comparison, the Kitaake genomic DNA was also sequenced.

Plasmid Construction. For genetic complementation, a 9.6-kb DNA fragment extending from 1,721 bp upstream of the *Bsr-k1* translation start to 609 bp downstream of its stop codon was amplified from genomic DNA isolated from Nipponbare rice by using primers digested with EcoRI and SaII and cloned into the vector pCambia1300 to generate the complementation construct. For overexpression, the full-length *Bsr-k1* cDNA sequence was amplified from Nipponbare and inserted into vector pCambia2300-35S-GFP, yielding construct p35S: *Bsr-k1-GFP*. For in vitro RIP

and RNA pull-down assays, the full-length *Bsr-k1* sequence and truncated *Bsr-k1* sequence were cloned into the pGEX-6p-1 vector to obtain prokaryotic expression recombinant constructs. For in vivo RIP assay, the 90-bp sequence of the 3×HA tag was inserted into the *Bsr-k1* complementation construct behind the translation start ATG to obtain construct pC1300: Native Promoter-3×HA-*Bsr-k1*.

Subcellular Localization. To determine the subcellular location of BSR-K1 in rice plants, we observed the roots of p35S: *Bsr-k1-GFP* plants (GFP was fused to the C terminus of *Bsr-k1*) under confocal microscopy (Nikon A1 i90; LSCM). To determine the subcellular location of BSR-K1 in *N. benthamiana*, we introduced constructs pC1300-35S-GFP, pC1300-35S-GFP-*Bsr-k1* (GFP was fused to the N terminus of *Bsr-k1*), and *Nls* and the pC1300-35S-GFP-*Bsr-k1* and *Nls* pair into *N. benthamiana* cells individually by agroinfiltration. To determine whether BSR-K1 was localized in cytomembrane, the constructs pC1300-35S-GFP-*Bsr-k1* and mCherry-cytomembrane were cotransformed into rice protoplasts. Fluorescence was examined 36 h post transformation under confocal microscopy.

Protein Expression and Purification. To overexpress and purify the GST-BSR-K1^{1-1,196 aa}, GST-BSR-K1^{1-288 aa}, and GST-BSR-K1^{1-105 aa} fusion proteins, the *E. coli* BL21 codon-positive strain was transformed with the corresponding prokaryotic expression recombinant constructs. When cell density reached an OD₆₀₀ of 0.6, 1 mM isopropyl-β-D-thiogalactopyranoside was added to induce expression, and the culture was shifted to 28 °C for 8 h. The expressed GST-fusion proteins were purified using glutathione Sepharose 4B (Amersham Biosciences) according to the manufacturer's instructions.

In Vitro and in Vivo RIP Assays. The in vitro RIP assay was performed as previously described with modifications (37). Briefly, the total RNA (300 μg) extracted from Kitaake plants was diluted with 900 μL of ChIP dilution buffer. Thirty microliters of glutathione-Sepharose beads (Amersham Biosciences) for each RIP sample were washed five times with 1 mL of binding/washing buffer (150 mM NaCl, 20 mM Tris HCl, pH 8.0, 2 mM EDTA, 1% Triton X-100, and 0.1% SDS), resuspended in 50 μL of binding/washing buffer, and then added to mixtures containing diluted total RNA/GST-BSR-K1 or total RNA/GST. The samples were incubated for 3 h at 4 °C and were washed six times with binding/washing buffer. Then RIP elution buffer was added to elute the protein-RNA complexes. The eluted samples were subjected to RNA extraction using TRIzol reagent (Ambion). The extracted RNA samples were further treated with the Turbo DNase Kit (Ambion) to remove DNA contamination and were cleaned with an RNeasy MinElute Kit (Qiagen) followed by sequencing (Shanghai Biotechnology Corporation).

For the in vivo RIP assay, 10-d-old seedlings (3 g) were treated with 0.5% formaldehyde for cross-linking, ground into a fine powder in liquid nitrogen, and suspended in 25 mL of extraction buffer [1.4 mM KH₂PO₄, 8 mM Na₂HPO₄, 140 mM NaCl, 2.7 mM KCl (pH 7.4), 0.5% Triton X-100, 1 mM PMSF, 1% protease inhibitor mixture (Sigma-Aldrich), and 20 units/mL RNase inhibitor]. The extract was centrifuged for 10 min at 16,000 × g at 4 °C, and the supernatant was transferred to a fresh tube. The 3×HA-BSR-K1 fusion protein complexes were then immunoprecipitated with anti-HA antibody using the Pierce HA Tag IP/Co-IP Kit (Thermo Scientific) following the manufacturer's instructions. The immunoprecipitated protein

complexes were subjected to RNA extraction as described for the in vitro RIP assay. The extracted RNA was dissolved with 15 μ L water and used for reverse transcription.

RNA Pull-Down Assay. In vitro, a DNA template containing an RNA polymerase promoter site was transcribed into RNA using the MEGAscript Kit (Ambion) following the manufacturer's instructions. A single desthiobiotinylated cytidine bisphosphate was attached to the 3' end of the RNA strand using the Pierce RNA 3' End Desthiobiotinylation Kit (Thermo Scientific). We then used the Pierce Magnetic RNA-Protein Pull-Down Kit (Thermo Scientific) to perform the RNA pull-down assay. Briefly, 50 pmol of biotinylated *OsPAL1* RNA in RNA structure buffer [10 mM Tris (pH 7), 0.1 M KCl, 10 mM MgCl₂] was heated to 95 °C for 2 min and then was slowly cooled to room temperature to allow proper secondary structure formation. Folded RNA was bound to the beads to orient the RNA for protein binding. RNA-bound beads were then equilibrated in protein-RNA binding buffer before the GST-BSR-K1 fusion protein was added. The samples were incubated at 4 °C with rotation for 60 min, and beads were then washed five times with wash buffer and boiled in SDS buffer. The recovered proteins were detected by Western blot with the α -GST antibody (Clontech).

Determination of mRNA Turnover Rate. The mRNA turnover rate was evaluated by the abundance of 5' and 3' ends of mRNA as

described previously (28). Briefly, three independent wild-type Kitaake and *bsr-k1* replicate samples were used for total RNA extraction. The total RNA was then subjected to reverse transcription with the reverse primers for each fragment, followed by qRT-PCR analysis as described previously (28).

RNA Extraction and qRT-PCR Analyses. Total RNA was extracted from rice plant tissues using TRIzol reagent (Ambion) according to the manufacturer's instructions. The total RNA was treated with DNase I (Thermo Scientific), and 1 μ g of total RNA was used for cDNA synthesis with SuperScript III (Thermo Scientific). The qRT-PCR was performed using a Bio-Rad CFX96 Real-Time System coupled to a C1000 Thermal Cycler (Bio-Rad). The transcript levels of genes were normalized to the transcript level of the reference *Ubiquitin 5 (Ubiq5)* gene. The primers used for qRT-PCR are listed in Dataset S6.

Determination of Total SA and Lignin Contents in Rice. Determination of total SA and lignin contents was performed by Bai Hui Biotechnology Co. Ltd at Chengdu, China, using the ultra-high performance liquid chromatography-triple quadrupole mass spectrometry (UPLC-MS/MS) method and the acid detergent lignin method. Each sample was measured with three biological repeats.

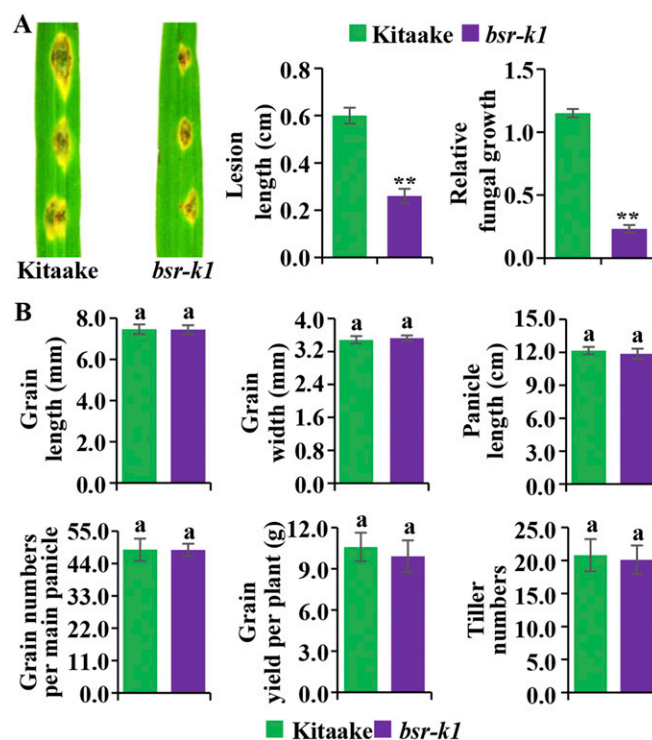


Fig. S1. Punch inoculation and comparison of the major agronomic traits of Kitaake and *bsr-k1* plants. (A) Photographs of representative leaves were taken 7 dpi with the spore mixture of seven Kitaake-compatible blast isolates. Statistical analyses of the disease lesion length (mean \pm SD, $n > 10$) and relative fungal growth (mean \pm SEM, $n = 3$) were performed on inoculated leaves. (B) Comparison of major agronomic traits of the *bsr-k1* mutant and wild-type Kitaake. Error bars represent mean \pm SD ($n > 30$). The same letter above bars indicates same statistical group ($P > 0.05$, Tukey's multiple comparison test).

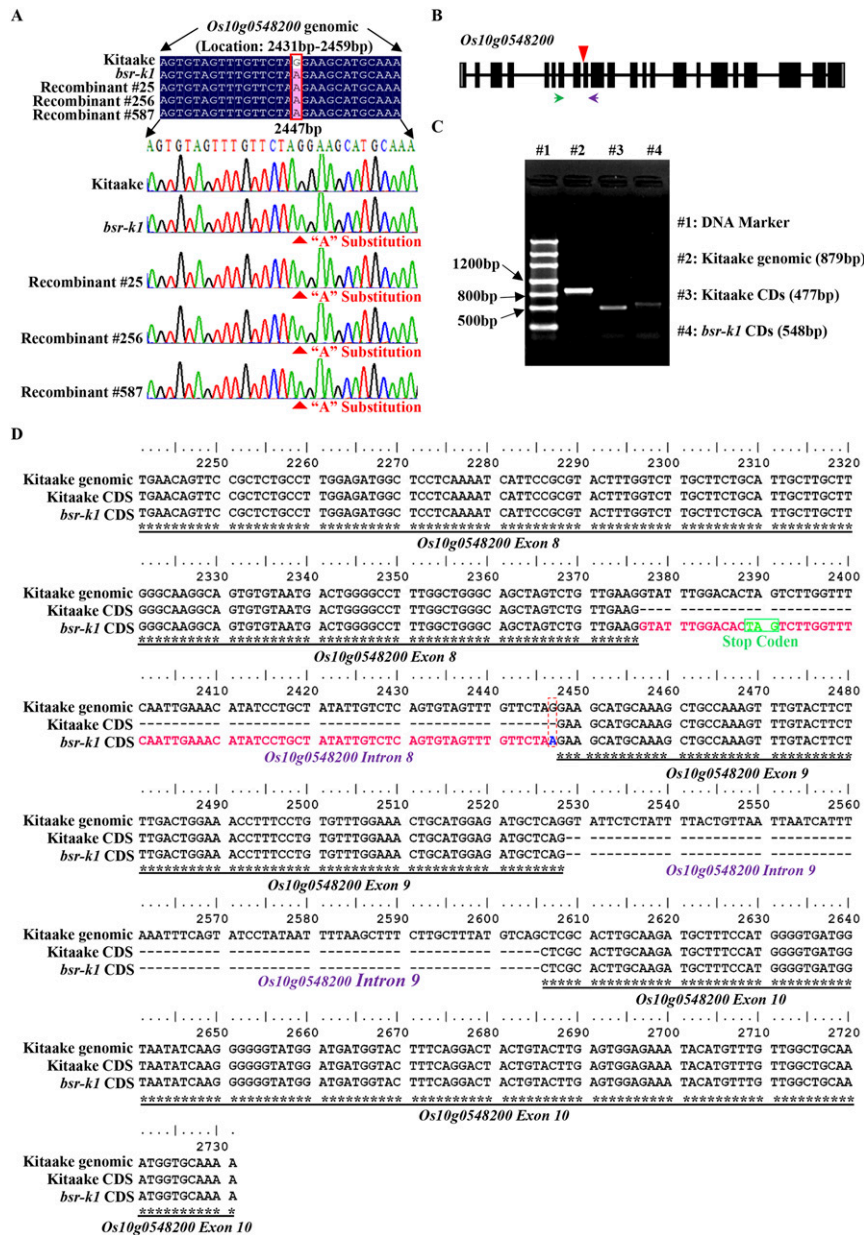


Fig. S2. Sequence verification of the mutation site in three recombinant lines with enhanced disease resistance and comparison of *Os10g0548200* cDNAs between Kitaake and *bsr-k1*. (A) The recombinants #25, #256, and #587 that exhibited high-level resistance were derived from the F₂ populations of Joden × *bsr-k1*. The DNA samples extracted from these three recombinant lines were subjected to PCR-based sequencing. (Upper) Sequence fragments containing the 2,447 position of the *Os10g0548200* gene. The three recombinants show a base change from G to A in position 2,447 of *Os10g0548200*. (Lower) The chromatograms of the sequences. (B) Primers for analysis of the partial cDNAs of *Os10g0548200* are depicted as arrows in the schematic drawing. The single-nucleotide substitution (G2447 → A2447) in *bsr-k1* is indicated by a red arrowhead. (C) Partial cDNAs of *Os10g0548200* amplified from wild-type Kitaake and the *bsr-k1* mutant, respectively, were separated in an agarose gel. The DNA fragment amplified from Kitaake genomic DNA by the same primer pair was used as a control. The amplified fragments are shown as indicated. (D) Alignment of the partial *Os10g0548200* cDNA sequences derived from Kitaake and *bsr-k1*. The corresponding genomic sequence of Kitaake is also included as a control for this alignment analysis. An insertion of a 71-bp intronic sequence in the cDNA of *bsr-k1* *Os10g0548200* is highlighted in red, and the stop codon causing premature termination of BSR-K1 is indicated in green.

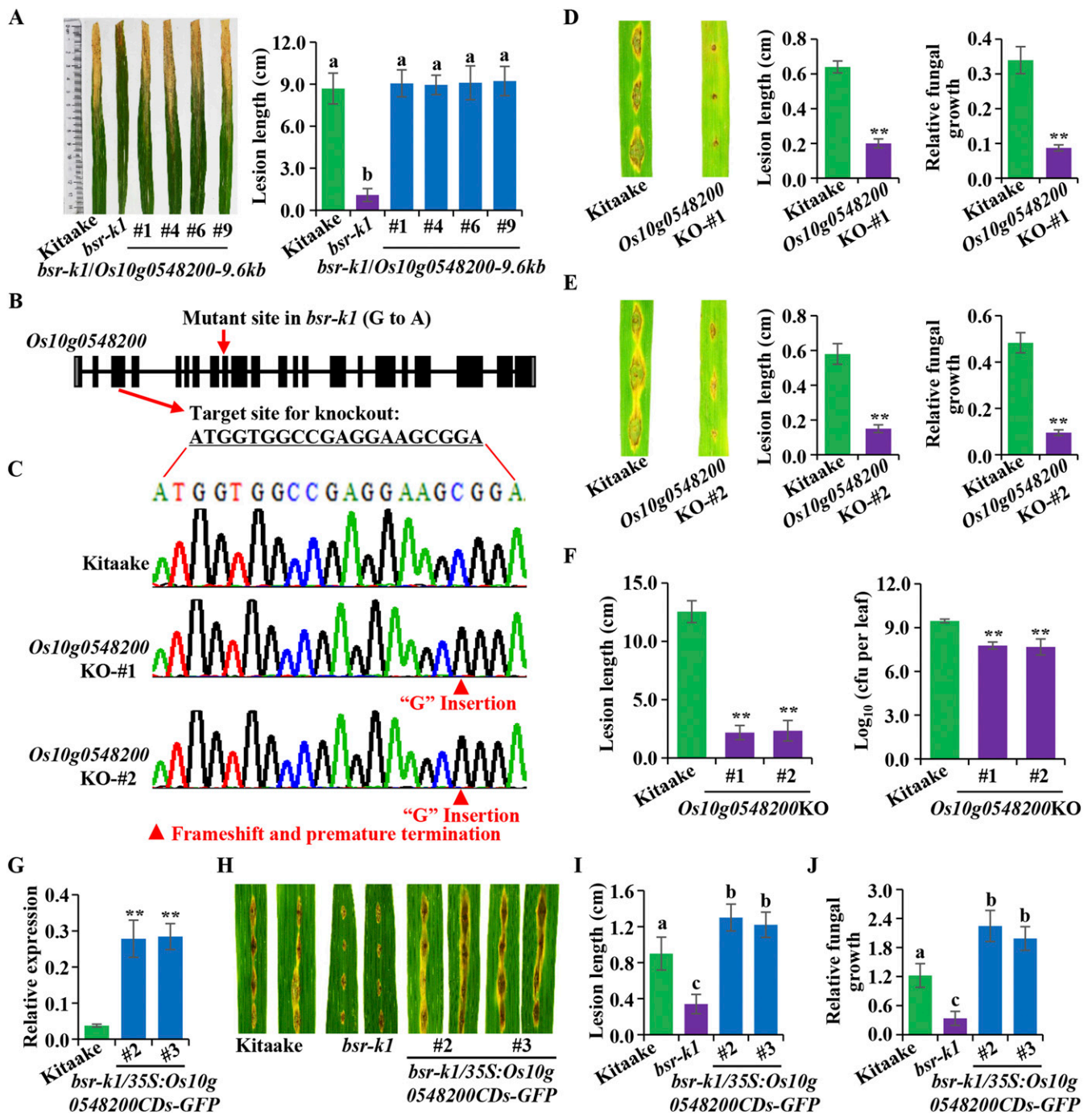


Fig. S3. Blast- and bacterial blight disease-resistance tests of *Os10g0548200* complemented, KO, and overexpression plants. (A) Bacterial blight disease-resistance test of *Os10g0548200* complemented lines. (Left) Photographs of representative leaves were taken 14 dpi with the Xoo P6 (Philippine race 6) isolate. (Right) Statistical analyses of the lesion length (mean \pm SD, $n > 10$) were performed on inoculated leaves. Different letters above bars indicate significant differences ($P < 0.05$, Tukey's test). (B) The target site designed for knocking out the *Bsr-k1* gene by the CRISPR/Cas9 system. The mutant site in *bsr-k1* (G to A) is also indicated. (C) DNA-sequencing chromatograms of two independent *Os10g0548200*KO lines. The two independent *Os10g0548200*KO lines show the same mutation, a G insertion, which leads to a frameshift and premature termination in the BSR-K1 coding in the cDNA of *Os10g0548200*, as indicated. (D and E) Determination of the resistance of *Os10g0548200*KO-#1 (D) and *Os10g0548200*KO-#2 (E) plants to blast disease. Photographs of representative leaves were taken 7 dpi with *M. oryzae*. Statistical analyses of the disease lesion length (mean \pm SD, $n > 10$) and relative fungal growth (mean \pm SEM, $n = 3$) were performed on inoculated leaves. (F) Determination of resistance of *Os10g0548200*KO-#1 and #2 plants to bacterial blight disease. Lesion length (Left) and bacterial population (Right) were measured at 2 wk after inoculation with the P6 isolate. (G) qRT-PCR detection of the expression level (mean \pm SEM, $n = 3$) of *Os10g0548200* in two overexpression lines ($**P \leq 0.01$, two-sided unpaired *t* test). (H) Punch inoculation of Kitaake, *bsr-k1*, and two independent *Os10g0548200* overexpression plants. Pictures were taken 7 dpi with *M. oryzae*. (I and J) Lesion length (I) and fungal growth (J) were measured on inoculated leaves. Different letters above bars indicate different statistical groups ($P < 0.05$, Tukey's test). Three independent experiments were repeated with similar results.

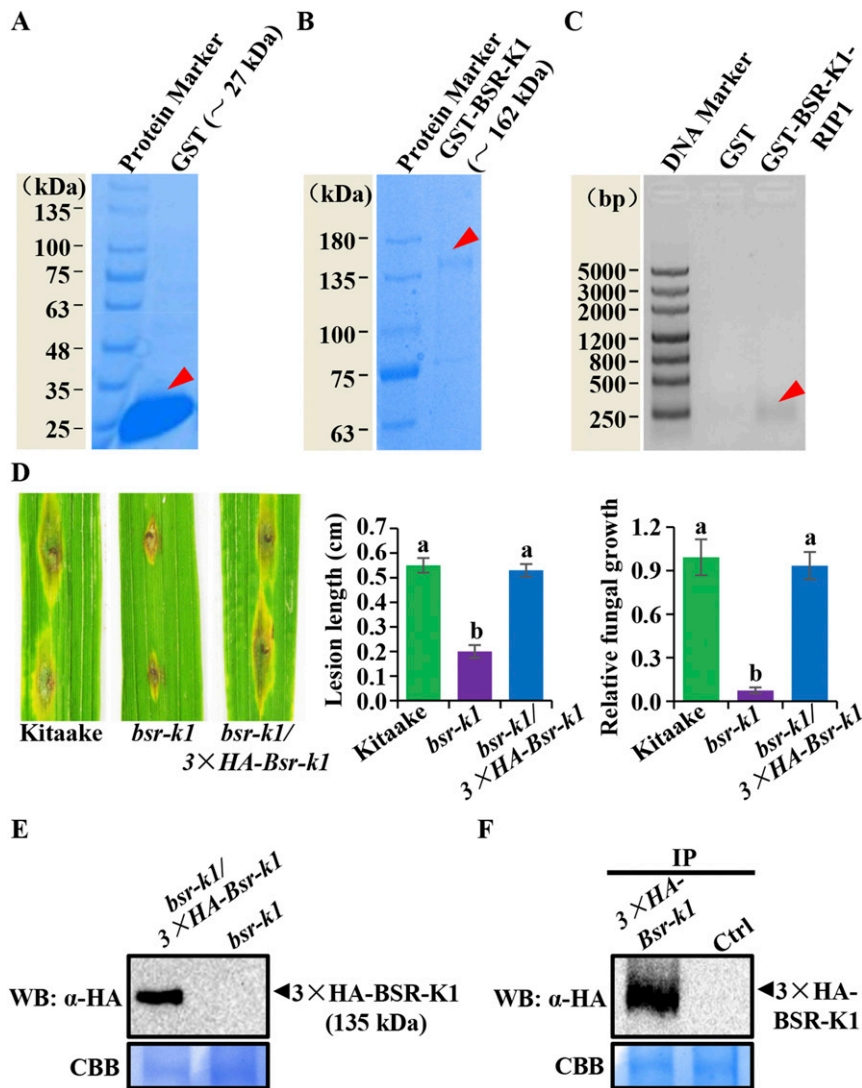


Fig. S5. In vitro RIP assays of BSR-K1 protein and detection of the 3xHA-BSR-K1 fusion protein in the *bsr-k1* mutant. (A and B) Detection of the GST protein (A) and the recombinant GST-BSR-K1 protein (B) purified from *E. coli*, by Coomassie brilliant blue staining. (C) Detection of RNA precipitated with GST-BSR-K1. The GST-BSR-K1 protein and GST protein (as a control) were each incubated with total RNA prepared from Kitaake rice leaves for 3 h at 4 °C, washed six times, and then subjected to RNA extraction. The extracted RNA was visualized after agarose electrophoresis. (D, Left) Punch inoculation of Kitaake, *bsr-k1*, and *bsr-k1/3xHA-Bsr-k1* plants. Photographs of representative leaves were taken 7 dpi with *M. oryzae*. Statistical analyses of lesion lengths (mean \pm SD, $n > 10$) (Center) and relative fungal growth (mean \pm SEM, $n = 3$) (Right) were performed on the inoculated leaves. (E) Western blot analysis with anti-HA to detect the 3xHA-BSR-K1 fusion protein in the transgenic plants. (F) Detection of 3xHA-BSR-K1 protein in the immunoprecipitated samples of *3xHA-Bsr-k1* transgenic plants. Input proteins were stained with Coomassie brilliant blue (CBB) for loading control. IP, immunoprecipitate.

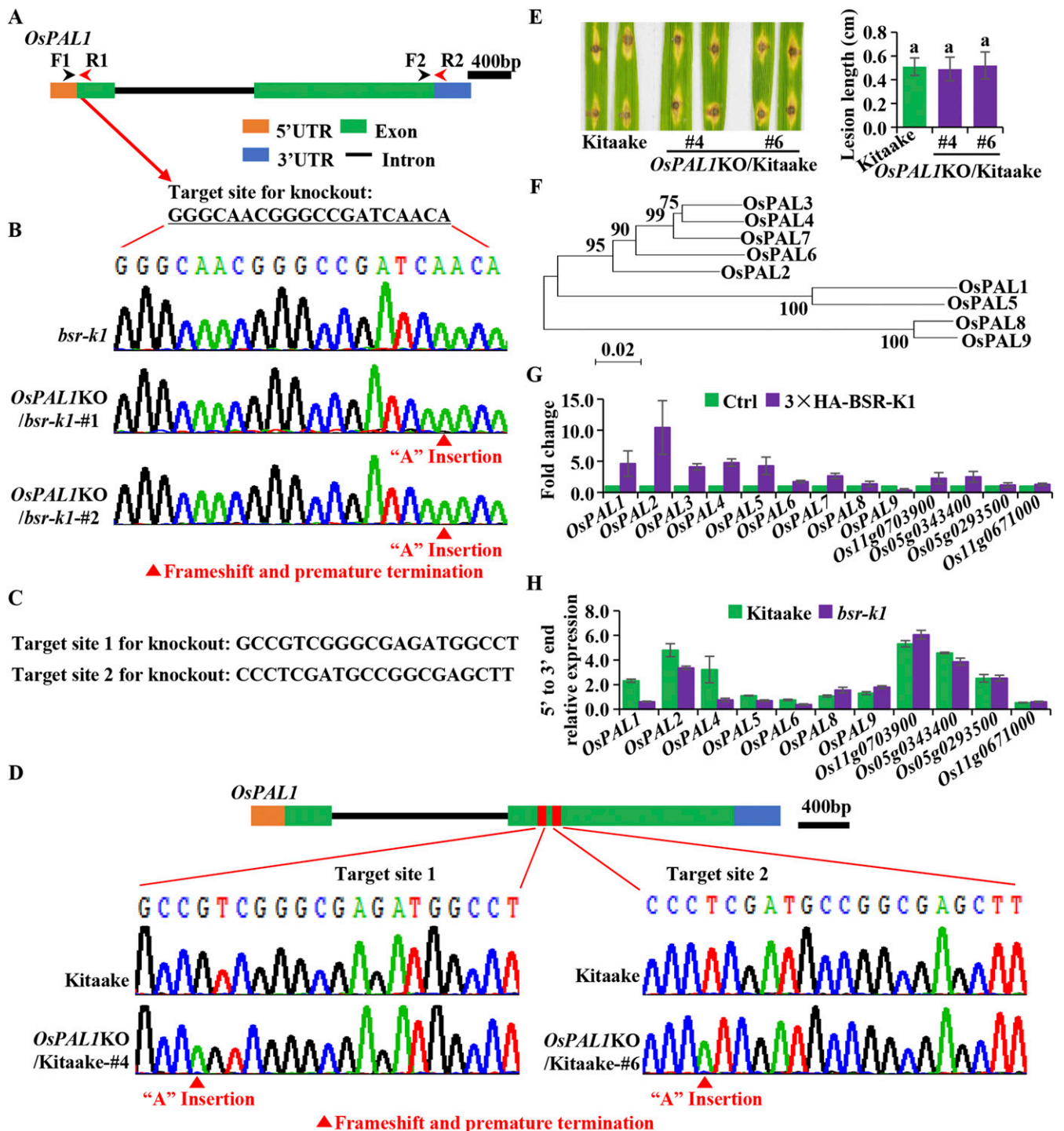


Fig. S6. CRISPR/Cas9-mediated knockout of *OsPAL1* in *bsr-k1* and Kitaake, binding to BSR-K1, and mRNA turnover rate of *OsPAL* genes. (A) A schematic drawing of the locations of qRT-PCR primers for the detection of *OsPAL1* turnover rate. Exons, intron, 5' TR, and 3' UTR regions of the *OsPAL1* gene are shown as indicated. The R1 and R2 reverse primers for each fragment were used to prime separate cDNA synthesis reactions, and the F1/R1 and F2/R2 primer pairs were used for determination of the abundances of 5' and 3' ends, respectively. (B) Verification of the *OsPAL1KO* lines in the *bsr-k1* mutant by PCR-based sequencing. The target site designed for knocking out the *OsPAL1* gene by the CRISPR/Cas9 system is shown above DNA-sequencing chromatograms. The two independent *OsPAL1KO* lines (*OsPAL1KO/bsr-k1-#1* and *-#2*) show the same mutation, an A insertion, which leads to a frameshift and premature termination in the *OsPAL1* protein as indicated. (C) Two independent target sites designed for knocking out the *OsPAL1* gene in Kitaake by the CRISPR/Cas9 system. (D) Verification of the *OsPAL1KO* lines in Kitaake by PCR-based sequencing. The two target sites designed for knocking out the *OsPAL1* gene in Kitaake are shown as indicated. The two representative transgenic lines (abbreviated as *OsPAL1KO/Kitaake-#4* and *OsPAL1KO/Kitaake-#6*, respectively) both contain an A insertion. (E) Punch inoculation of wild-type Kitaake, *OsPAL1KO/Kitaake-#4*, and *OsPAL1KO/Kitaake-#6* plants. (Left) Photographs of representative leaves were taken 7 dpi with the blast isolate Zhong1. (Right) Statistical analyses of lesion lengths (mean \pm SD, $n > 10$) were performed on the inoculated leaves. (F) Phylogenetic analysis of the *OsPAL1* homologous genes using Mega5.1 (Molecular Evolutionary Genetics Analysis). Bootstrap values are indicated beside each branch. (G) Enrichment of *OsPAL* genes and other immunity-related genes detected in RIP-seq (Dataset S3C) in $3\times$ HA-*Bsr-k1* plants as detected by qRT-PCR. The enrichment was calculated as the fold change in the abundance of RNA immunoprecipitated in $3\times$ HA-*Bsr-k1* plants compared with Kitaake. *Os11g0671000* was used as the negative control. (H) mRNA turnover rate (mean \pm SEM, $n = 3$) of *OsPAL* genes and other immunity-related genes detected in the RIP-seq (Dataset S3C) in *bsr-k1* and Kitaake.

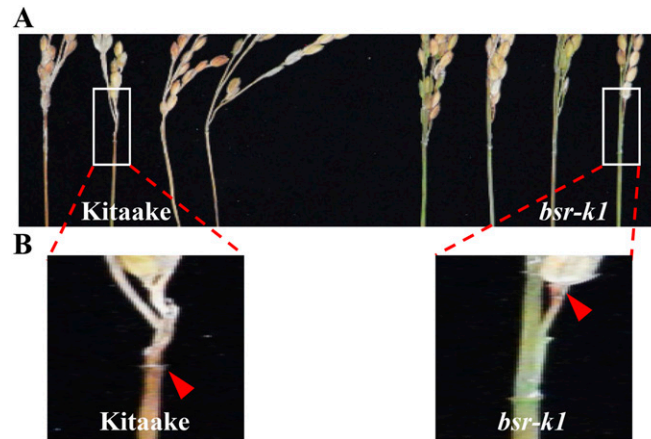


Fig. 57. Determination of panicle blast disease resistance in Kitaake and *bsr-k1* plants. (A) Determination of panicle blast disease resistance in wild-type Kitaake and the *bsr-k1* mutant. The representative panicles are derived from the plants shown in Fig. 5A. Images in the white squares are enlarged and shown in B with the inoculated phenotypes (arrowheads). The *bsr-k1* mutant exhibits enhanced panicle blast disease resistance compared with wild-type Kitaake.

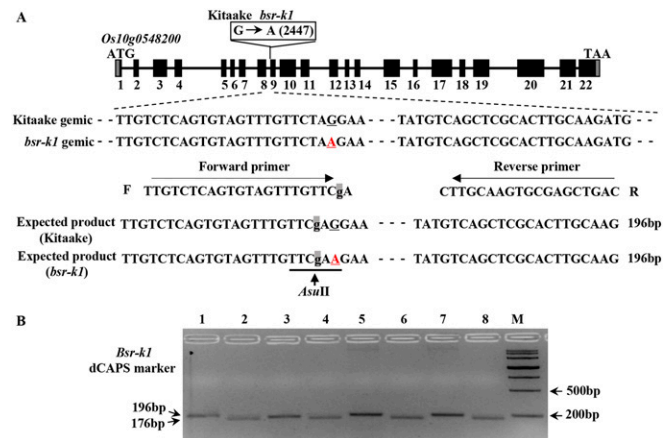


Fig. 58. Developing a dCAPS (derived Cleaved Amplified Polymorphic Sequence) marker for determination of the *bsr-k1* genotype when the *bsr-k1* allele was introduced into elite rice cultivars. (A) The dCAPS marker with a specific recognition site by the restriction enzyme *Asu*II (TTCGAA) in *bsr-k1* but not in *Bsr-k1* was designed. The primer sequences and expected products are shown. (B) Genotyping the *bsr-k1* locus using the dCAPS marker. Lane 1: DNA from wild-type Kitaake plants. Lane 2: DNA from *bsr-k1* plants. Lane 3: Shuhui498. Lane 4: Shuhui498^{*bsr-k1/bsr-k1*}. Lane 5: Minghui63. Lane 6: Minghui63^{*bsr-k1/bsr-k1*}. Lane 7: Mianhui725. Lane 8: Mianhui725^{*bsr-k1/bsr-k1*}. M, DNA size markers.

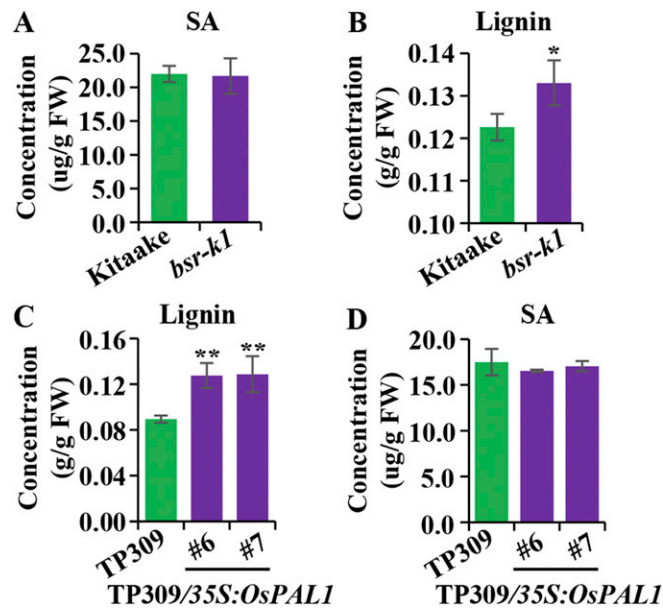


Fig. S9. Determination of SA and lignin contents in Kitaake, *bsr-k1*, and *OsPAL1* overexpression plants. (A) SA content (mean \pm SD, $n = 3$) of Kitaake and *bsr-k1* plants. (B) Lignin content (mean \pm SD, $n = 3$) of Kitaake and *bsr-k1* plants ($*P \leq 0.05$, two-sided unpaired *t* test). (C) Lignin content (mean \pm SD, $n = 3$) of *OsPAL1* overexpression plants and wild-type TP309 ($**P \leq 0.01$, two-sided unpaired *t* test). (D) SA content (mean \pm SD, $n = 3$) of TP309, TP309/35S:*OsPAL1*-#6, and -#7 plants.

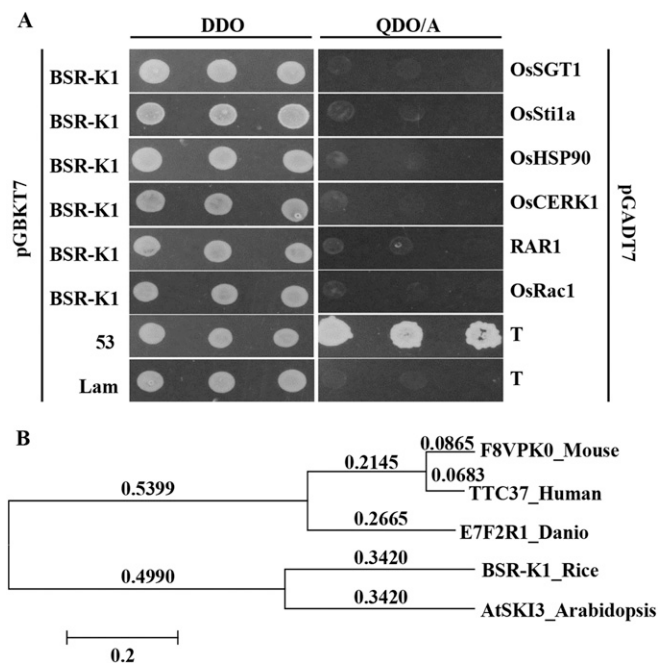


Fig. S10. Detection of interaction between BSR-K1 and the rice defense complex in yeast and phylogenetic analysis of BSR-K1 protein. (A) The full-length coding sequences of OsSGT1, OsSti1a, OsHSP90, OsCERK1, RAR1, and OsRac1 were individually cloned into the pGADT7 vector to obtain constructs AD-OsSGT1, AD-OsSti1a, AD-OsHSP90, AD-OsCERK1, AD-RAR1, and AD-OsRac1. These constructs were each cotransformed with the pGBKT7-BSR-K1 vector into yeast. pGBKT7-53/pGADT7-T and pGBKT7-Lam/pGADT7-T, representing positive and negative interactions, were also included in this test. The positive transformants were spotted on double-dropout medium (SD/-Leu/-Trp; DDO) and quadruple-dropout medium supplemented with Aureobasidin A (Aba) (SD/-Ade/-His/-Leu/-Trp/Aba; QDO/A) plates. Growth of cotransformed yeast cells in the QDO/A medium indicates protein-protein interactions in yeast. (B) Phylogenetic analysis of BSR-K1 with TPR proteins from different organisms using Mega5.1. Bootstrap values are indicated beside each branch.

Dataset S1. Genetic analyses of the *bsr-k1* locus against blast isolate 99-20-2

[Dataset S1](#)

Dataset S2. The 11 predicted genes in the candidate region between ID13 and ID16

[Dataset S2](#)

Dataset S3. GST-BSR-K1-associated RNAs in the two RIP-seq datasets

[Dataset S3](#)

Dataset S4. Main agronomic traits and yields of three rice breeding cultivars carrying homozygous *bsr-k1*

[Dataset S4](#)

Dataset S5. *M. oryzae* isolates used for screening Kitaake-compatible blast isolates

[Dataset S5](#)

Dataset S6. Primers used in this study

[Dataset S6](#)